Early Results from SSGSS: The *Spitzer*-SDSS-*GALEX* Spectroscopic Survey

Benjamin D. Johnson[1], David Schiminovich[2], Matthew O'Dowd[2], Kirsten Meder[2], Marie Treyer[3] for the SSGSS Team

ABSTRACT

SSGSS is a Spitzer Legacy program of IRS observations of 101 galaxies uniformly selected from the SDSS (median redshift ~ 0.08). The comprehensive UV through IR imaging and spectroscopy of a representative sample of galaxies in the local universe will provide an ideal dataset for the testing of models that self consistently treat stellar populations, dust absorption, and dust emission. The IRS slits are well-matched to the SDSS spectroscopic aperture, and in the most cases sample the majority of emission of each galaxy. Mid-IR indicators of PAH abundance, dust temperature and luminosity, and AGN activity derived from the SSGSS data may be compared to optical and UV indicators of star formation, stellar mass, dust attenuation, metallicity, and AGN activity. As an example, we explore how PAH feature strength ratios vary with optical diagnostics of HII regions, and the variation of the IR continuum shape with the stellar population 'age' in galaxies. We also determine a simple scaling between the 7.7μm PAH feature emission strength and the optically derived star formation rate.

Subject headings: galaxies: ISM — infrared: galaxies — infrared: ISM — ISM: dust, extinction — ISM: structure

1. Introduction

The $\sim$500,000 galaxies of the SDSS spectroscopic galaxy sample constitute an extremely powerful data set that has and will form the basis for much of our knowledge of galaxy

[1]Institute of Astronomy, University of Cambridge, Madingley Rd, Cambridge CB3 0HA, UK

[2]Department of Astronomy, Columbia University, New York, NY 10027

[3]California Institute of Technology, MC 405-47, 1200 East California Boulevard, Pasadena, CA 91125

properties in the local universe. It has been used, often in combination with models of galaxy stellar populations, to advance our understanding of the star formation rates (SFR) (Brinchmann et al. 2004), star formation histories (SFH), AGN activity (Kauffmann et al. 2003a), dust attenuations and stellar masses of galaxies, to determine the fully representative distributions of basic observable quantities such as color and luminosity (Blanton et al. 2003), and to investigate the relation of these properties to galaxy environment and morphology (e.g., Balogh et al. 2004). This new knowledge is driving the development and refinement of models of galaxy evolution.

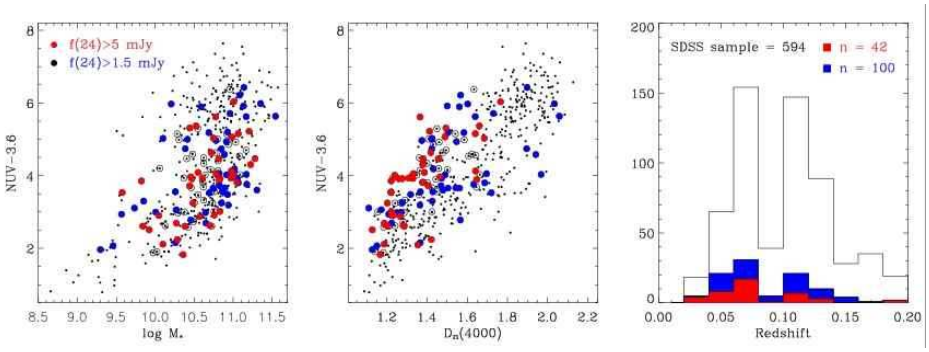

Fig. 1.— The SSGSS 'bright' sample is shown in red, the SSGSS 'faint' sample in blue, overplotted on the SDSS Lockman Hole galaxies of Johnson et al. (2006).

We remain in need of high quality mid-IR SEDs and spectroscopy for a representative sample in the local universe that may be used to more accurately constrain galaxy properties and serve as a comparison sample and calibrator for high-redshift and extreme-galaxy studies (e.g., Armus et al. 2007). We have used the *Spitzer* IRS to obtain spectra of a representative sample of 101 galaxies imaged by *GALEX*, SDSS and *Spitzer*/SWIRE. We will use these data to study the global properties of SDSS galaxies using atomic and molecular nebular diagnostics measured from IR to UV.

Among the key questions that we will address are: (1) How can a full complement of UV optical and mid-IR photometry and spectroscopy be used to determine physical properties of "normal" galaxies such as SFR, SFH, dust content, AGN activity, and nebular conditions? (2) How can the combination of optical+mid-IR spectroscopic diagnostics be used to probe the ISM structure (i.e. molecular clouds versus diffuse ISM) and the relative heating of dust by young and old stars, and AGN, in galaxies of different types? (3) What can we learn from the combination of optical and mid-IR signatures about AGN activity in bulges, Seyfert, LINERS, etc.?

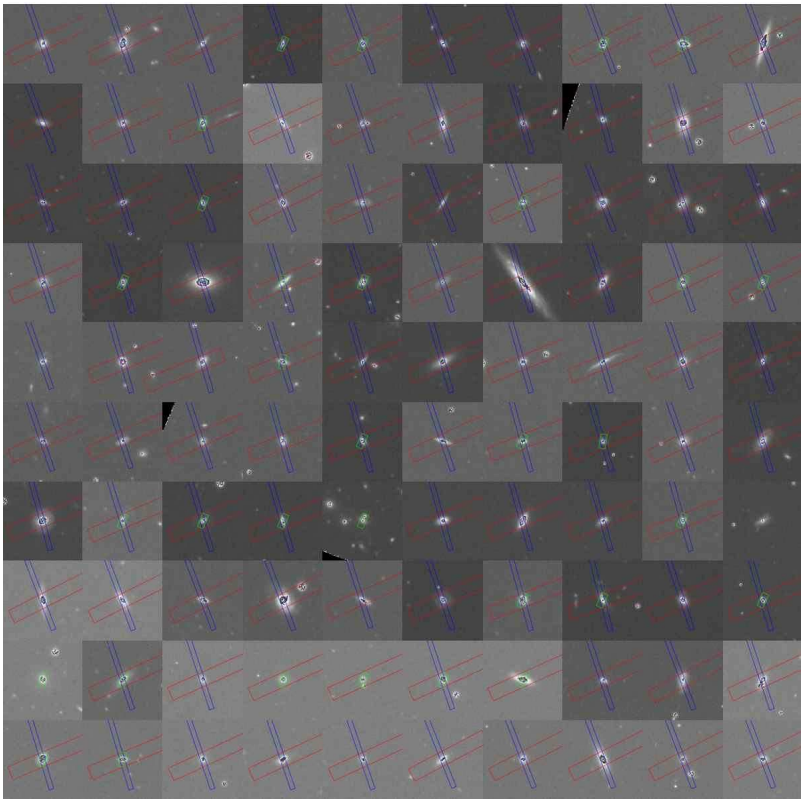

Fig. 2.— The SH (*green*), SL (*blue*), and LL (*red*) IRS slits overlayed on SDSS r band images for the SSGSS sample. Each cutout is 60″ square.

2. The SSGSS Program: Sample and Observations

SSGSS targets are selected from the sample of Johnson et al. (2006, 2007). These galaxies, for which there exists SDSS imaging and spectroscopy, are in a ~ 9 deg.^{2} region of the Lockman Hole. The SDSS spectroscopic selection is of galaxies with $r < 17.7$ mag. In Figure 1 we show the properties of the SSGSS sample compared to the full Johnson et al. (2006) sample. The SSGSS sample is representative of galaxies in the SDSS main spectroscopic sample, covering two orders of magnitude in stellar mass, color, and dust attenuation. Along with SDSS imaging and spectroscopy, all SSGSS targets have been observed with deep (15-30ks) f ($\lambda \sim 1520$Å) and n ($\lambda \sim 2250$Å) band *GALEX* pointings, and with the *Spitzer* IRAC and MIPS instruments from 3.6 to 160μm by the SWIRE survey.

The SSGSS observations with IRS consist of Short-Low (SL, 5-18μm) and Long-Low (LL, 15-40μm) spectroscopy and IRS 16μm "peak-up" imaging of all 101 program galaxies. For the 'bright' sample (33 galaxies) we have obtained additional Short-High (SH, 8-19μm) spectroscopy. In Figure 2 the IRS slits – well matched to the SDSS spectroscopic aperture

– are shown overlayed on SDSS r band images.

3. SSGSS Spectra (and Images)

Extraction of the SSGSS spectra with SPICE was performed to produce 1-d spectra. The spectra from different slit positions were combined and the spectra from different orders and modules were stitched together, using a weighted median in the regions of overlap (relative normalization was generally excellent and no re-normalizations were applied).

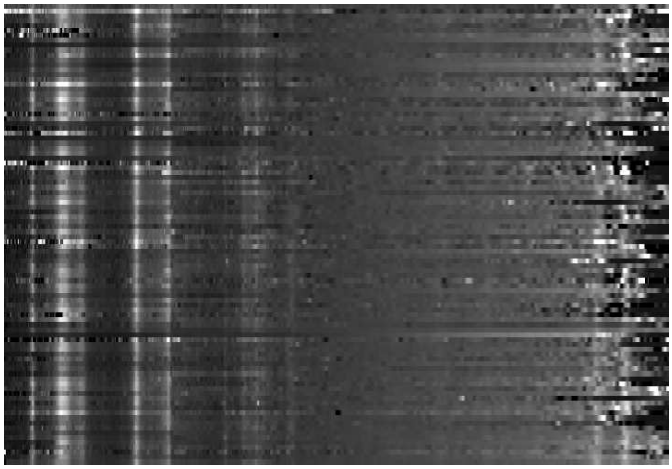

Fig. 3.— The deredshifted SSGSS low resolution (SL+LL) 1-d spectra for all 101 galaxies. Wavelength increases linearly to the right, different galaxies are shown on each line, $n - r$ increasing to the top. The prominent 7.7 and 11.3μm PAH features are easily visible, as well as a number of other features including NeIII and SIII.

In Figure 4 we show the SSGSS *Spitzer* spectra and the ancillary imaging and SDSS spectra for a selection of 3 galaxies, including a merger, an early-type galaxy, and a star-forming spiral galaxy that is more typical of the SSGSS sample.

3.1. Composite Spectra

The stacked low resolution spectra (normalized by 20-24μm flux) show numerous features, many of which are detectable in the majority of the individual spectra. These include H_2 and PAH emission, and nebular features including two lines of SIII, NeIII, ArII, and OIV. The SH staked spectra show three strong H_2 rotational lines, Ne nebular lines, and PAH features.

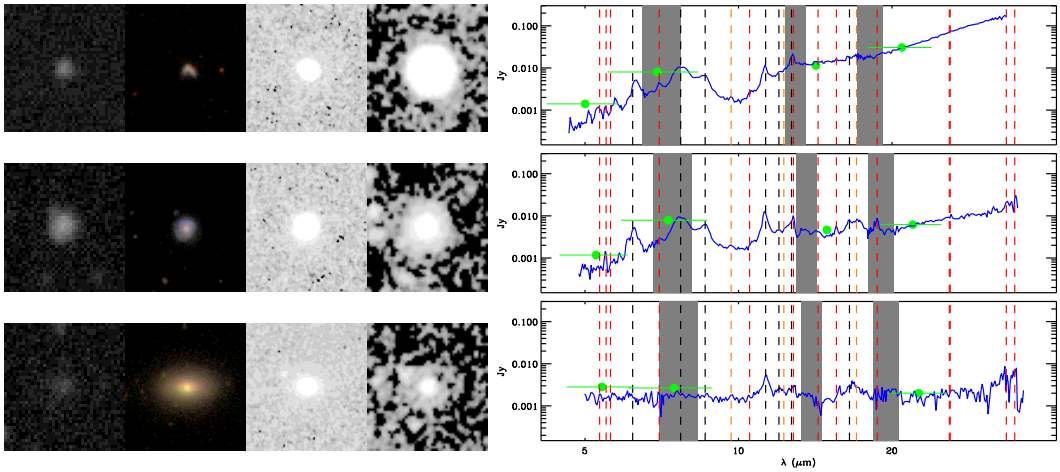

Fig. 4.— SSGSS data for a subset of 3 of the sample galaxies. **Left:** For each galaxy f, SDSS *gri* composite, 7.8, and 24μm SWIRE images (left to right) are shown. The images are 60" square. SDSS optical spectra are also available. **Right:**The SSGSS SL+LL spectra are shown with the SWIRE+SSGSS photometry (*green*) and the expected locations of spectral features (PAH, *black*; H_2, *orange*; Nebular, *red*) overplotted. Gray shaded regions show where order or module wavelength overlap occurs.

4. Preliminary Analysis

4.1. PAH Features as a Measure of SFR

An understanding of the Mid-IR spectra of galaxies is important for the use of this spectral region as an indicator of physical quantities in high-redshift studies and for extreme galaxy types. One avenue for such understanding is the comparison of Mid-IR spectral features, especially the PAH emission bands, to the more well understood optical indicators. We have used PAHFIT (Smith et al. 2007) to measure PAH (and other feature) strengths from the low-resolution SSGSS spectra.

In Figure 6 we show the ratio of the luminosity of the 7.7μm complex (including features with central wavelengths between 7.4 and 7.9 μm restframe) to the SFR derived from optical emission lines and photometry by (Brinchmann et al. 2004). The average value is $\langle \log(L_{7.7}/SFR_e) \rangle = 42.01$ erg s^{-1} $M_\odot{}^{-1}$ yr, with standard deviation of 0.25 dex. However, the scatter does seem to correlate with $D_n(4000)$, a coarse measure of the global SFH of the galaxy. UV photometry suggests that this is *not* simply a progression in the attenuation (i.e., that significant star formation is unobscured and therefore not represented in the Mid-IR for

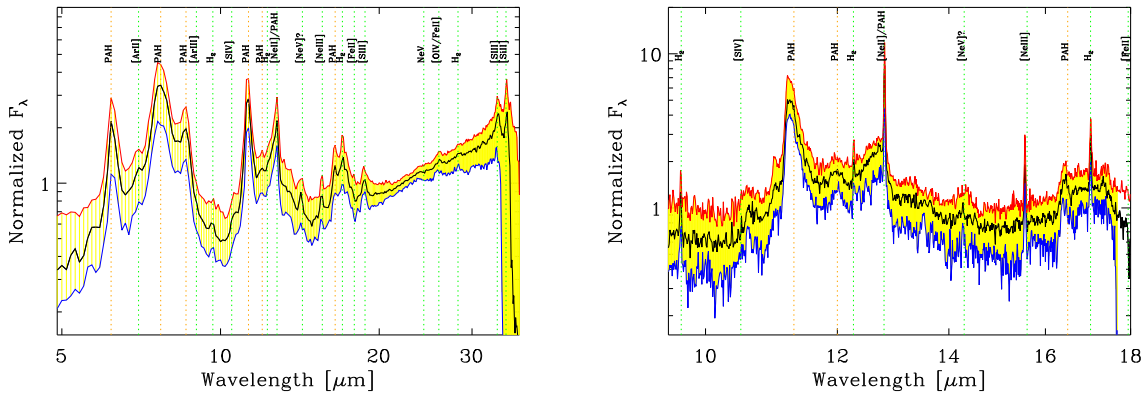

Fig. 5.— **Left:** Composite SL+LL spectrum of 93 galaxies, showing the median (*black*) and 16th (*blue*) and 84th (*red*) percentiles at each wavelength. Spectra are normalized by 20-24μm flux. **Right:**Composite SH spectrum of 33 galaxies, showing the median, 16th, and 84th percentiles at each wavelength, normalized by 13.6-13.8μm flux.

higher $D_n(4000)$ galaxies).

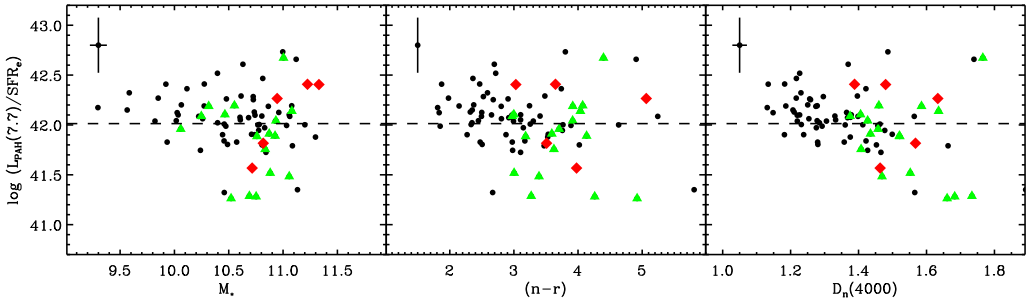

Fig. 6.— The ratio of the 7.7μm PAH complex luminosity (in erg/s) to the SFR (in $M_\odot \mathrm{yr}^{-1}$) determined by (Brinchmann et al. 2004) from SDSS emission lines and photometry, shown as a function of three other galaxy properties. These properties are, from left to right, the log of the stellar mass (in $M_\odot$) (M_*, Kauffmann et al. 2003b), $n-r$ band color, and $D_n(4000)$. The dashed line shows the average value for this ratio, and median error bars (dominated by the error in SFR_e) are shown in the top left of each panel. Galaxies with evidence for AGN activity are marked (*red diamonds*), as those with optical emission line ratios suggesting a mix of AGN and star formation (*green triangles*) (Kauffmann et al. 2003b).

4.2. PAH Ratios and Optical Nebular Lines

Variations in the PAH emission strength may be due not only to variations in SFR, but also to differences in the the PAH abundance and physical conditions. In particular, the the ratio of the 7.7 (C-C stretch) to 11.3 μm (C-H bending) PAH strengths varies between galaxies by more than an order of magnitude (Smith et al. 2007). In Figure 7 we show this ratio versus 2 optical emission line ratios that are sensitive to the ionization parameter and gas-phase metallicity within galaxies.

There is perhaps a very small trend of the PAH ratio with NII/Hα , but no evidence for a correlation with the OIII/Hβ line ratio. We will be able to use additional emission lines in the optical and MIR (including Ne and S lines) to further probe the physical conditions in galaxies with different PAH ratios (including several different PAH bands, such as the 6.2 micron band)

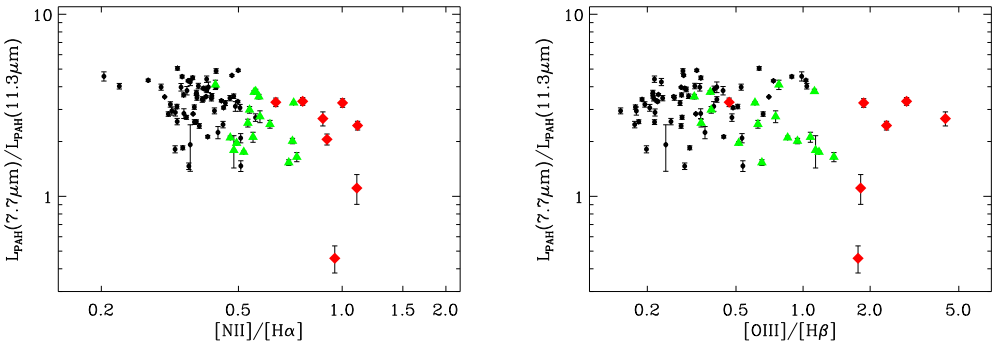

Fig. 7.— **Left:** Ratio of PAH feature strength vs. the NII/Hα optical emission line flux ratio. **Right:** Versus the OIII/Hβ line ratio. Colors are as in Fig. 6

4.3. The IR Continuum and Stellar 'Age'

Dust heated by different starlight intensities (diffuse dust vs. dust near photo-dissociation regions) will produce different IR conitinua. We investigate the degree to which the IR continuum shape depends on the galaxy type by plotting the IR spectral slope ($f_\nu \sim \nu^\alpha$) between 23 and 30μm against $D_n(4000)$, a coarse measure of the SFH of galaxies (Figure 8. Galaxies with large $D_n(4000)$ (more older stars) appear to have blue spectral slopes (which is indicative of lower dust heating intensity according to the models of (Draine & Li 2007). However, the lack of a strong correlation is in contrast to studies that suggest that the IR SED shape is strongly correlated with the SF activity in galaxies (Lonsdale Persson & Helou

1987, e.g.,). 70 and 160μm photometry and measured PAH strengths will provide further constraints on the dust heating and PAH abundance.

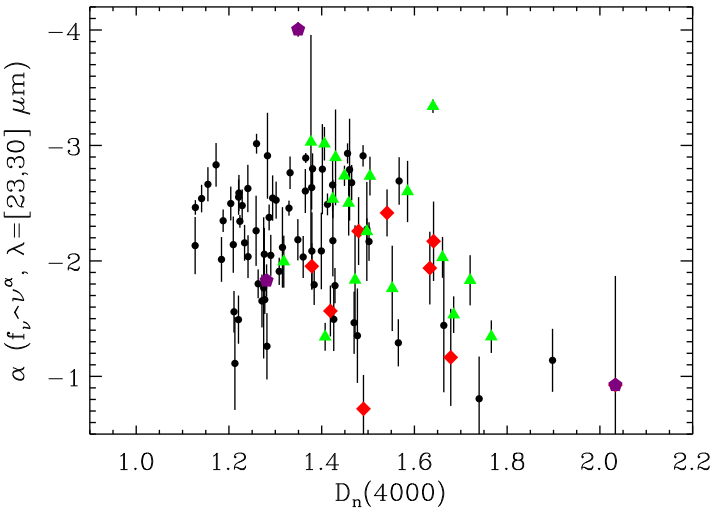

Fig. 8.— The 23-30μm continuum slope vs $D_n(4000)$. Colors are as in Fig. 6. The three galaxies of Fig. 4 are marked (*purple pentagons*).

5. Summary

- SSGSS has obtained *Spitzer* IRS SL and LL observations of 101 uniformly selected SDSS galaxies with GALEX and SWIRE observations. For 33 of these galaxies SSGSS has obtained SH spectroscopy. PAH features, nebular emission lines, H_2 emission lines, and the thermal dust continuum are all visible in individual and stacked spectra.

- The 7.7μm PAH emission luminosty correlates with the SFR as determined from optical emission lines with a scatter of 0.25 dex for this sample. The ratio of the 7.7μm to 11.3μm PAH emission varies by an order of magnitude, and 11.3μm (but not 7.7μm) PAH emission is detected in an early-type galaxy in the sample.

- IR continuum slopes appear to vary with the stellar content of galaxies, suggesting a relation between dust heating modes and SFH.

- The combined dataset including especially the IR continuum slopes and relative PAH strengths can be used to constrain the dust properties (heating intensity, PAH abundance) and the dust heating sources (AGN, young stars, old stars)

This work is based on observations made with the *Spitzer Space Telescope*, which is operated by the Jet Propulsion Laboratory (JPL), California Institute of Technology under NASA contract 1407. We gratefully acknowledge the SWIRE survey legacy team (PI: Lonsdale) for obtaining the Lockman field data and making it publicly available, the SDSS collaboration and the hard work of the MPA/JHU collaboration that constructed the value-added catalogs used in our analysis.

REFERENCES

Armus, L. et al. 2007, ApJ, 656, 148

Balogh, M. L., Baldry, I. K., Nichol, R., Miller, C., Bower, R., & Glazebrook, K. 2004, ApJ, 615, L101

Blanton, M. R. et al. 2003, ApJ, 594, 186

Brinchmann, J., Charlot, S., White, S. D. M., Tremonti, C., Kauffmann, G., Heckman, T., & Brinkmann, J. 2004, MNRAS, 351, 1151

Draine, B. T., & Li, A. 2007, ApJ, 657, 810

Johnson, B. D. et al. 2006, ApJ, 644, L109

—. 2007, ApJS, 644, 000

Kauffmann, G. et al. 2003a, MNRAS, 346, 1055

—. 2003b, MNRAS, 341, 33

Lonsdale Persson, C. J., & Helou, G. 1987, ApJ, 314, 513

Smith, J. D. T. et al. 2007, ApJ, 656, 770